Current Biology *17*, 1586–1594, September 18, 2007 DOI 10.1016/j.cub.2007.08.034

Report

Disruption of Intraflagellar Transport in Adult Mice Leads to Obesity and Slow-Onset Cystic Kidney Disease

James R. Davenport,[1] Amanda J. Watts,[2] Venus C. Roper,[1] Mandy J. Croyle,[1] Thomas van Groen,[1] J. Michael Wyss,[1] Tim R. Nagy,[2] Robert A. Kesterson,[3] and Bradley K. Yoder[1,*]
[1]Department of Cell Biology
[2]Department of Nutrition Sciences and
[3]Department of Genetics
University of Alabama at Birmingham
Birmingham, Alabama 35294

Summary

The assembly of primary cilia is dependant on intraflagellar transport (IFT), which mediates the bidirectional movement of proteins between the base and tip of the cilium. In mice, congenic mutations disrupting genes required for IFT (e.g., *Tg737* or the IFT kinesin *Kif3a*) are embryonic lethal, whereas kidney-specific disruption of IFT results in severe, rapidly progressing cystic pathology [1–3]. Although the function of primary cilia in most tissues is unknown, in the kidney they are mechanosenstive organelles that detect fluid flow through the tubule lumen [4]. The loss of this flow-induced signaling pathway is thought to be a major contributing factor to cyst formation [5–7]. Recent data also suggest that there is a connection between ciliary dysfunction and obesity as evidenced by the discovery that proteins associated with human obesity syndromes such as Alström and Bardet-Biedl localize to this organelle [8]. To more directly assess the importance of cilia in postnatal life, we utilized conditional alleles of two ciliogenic genes (*Tg737* and *Kif3a*) to systemically induce cilia loss in adults. Surprisingly, the cystic kidney pathology in these mutants is dependent on the time at which cilia loss was induced, suggesting that cyst formation is not simply caused by impaired mechanosensation. In addition to the cystic pathology, the conditional cilia mutant mice become obese, are hyperphagic, and have elevated levels of serum insulin, glucose, and leptin. We further defined where in the body cilia are required for normal energy homeostasis by disrupting cilia on neurons throughout the central nervous system and on pro-opiomelanocortin-expressing cells in the hypothalamus, both of which resulted in obesity. These data establish that neuronal cilia function in a pathway regulating satiety responses.

Results

Our understanding of ciliary function in adults is hindered by the midgestation lethality of intraflagellar transport (IFT) mutants and severe near-systemic pathology leading to early mortality in hypomorphic mutants [3, 9, 10]. To overcome this limitation, we utilized conditional null alleles of *Kif3a* and *Tg737* to systemically disrupt IFT by using a tamoxifen-inducible Cre recombinase expressed from the actin promoter (CAGG-creER [2, 11, 12]). The efficient deletion of *Tg737* and *Kif3a* and subsequent loss of cilia was confirmed by western blot and immunofluorescence (Figures 1A and B). Despite the absence of cilia, the mutants did not exhibit cystic kidneys, hydrocephalus, or the ductal abnormalities in the pancreas or liver at 16 weeks after tamoxifen injection (Figures 1C–1E, ad libitum fed). These phenotypes are normally present in the $Tg737^{orpk}$ hypomorphic mutants, in which cilia function is impaired from conceptus [13–15]. Although there were no overt biliary duct phenotypes, there was a liver pathology that was evident in ad libitum-fed mutants at 16 weeks after injection, and this pathology consisted of an increase in lipid content, as shown by oil red O staining (Figure 1D and see below). This phenotype is not seen in the liver of the $Tg737^{orpk}$ mutants. Cysts in the kidney and liver did eventually form in the conditional mutants. In the kidney, small cysts first became evident approximately six months after injection (Figure 1F). By one year, these cysts were severe and the kidneys had become markedly enlarged (Figure 1G). In contrast to the slow rate of cyst progression in the adult-induced mutants, the administration of tamoxifen to pregnant females at E17.5 caused rapid cyst development in the kidney during the perinatal period normally within 2 weeks of birth (Figure 1H).

Although significant cystic pathologies in the kidney and liver were not seen in adult-induced cilia mutants until 6 months after tamoxifen administration, both male and female adult *Kif3a* and *Tg737* conditional mutants exhibit an increase in body weight shortly after tamoxifen administration (Figures 2A–2D). In *Kif3a* and *Tg737* male and female mutants, the weekly food intake was markedly increased compared to control mice (Figures 2E–2F, Figures S1A–S1B in the Supplemental Data available online). The weight gain in these mutants was primarily due to hyperphagia, as evidenced by the data from pair-feeding studies. Although $Kif3a^{loxP/null}$; *CAGG-creER* (hereafter called Kif3a-cKO) mice fed ad libitum gained substantial weight, Kif3a-cKO mice pair fed to the control ($Kif3a^{loxP/wt}$; *CAGG-creER*, hereafter called Kif3a-cWT) did not exhibit a significant increase in weight compared to controls (Figure 2G, Figure S1C). In addition, we diet restricted Kif3a-cKO males to 4.0 g food/day, similar to the food consumption by control littermates over a similar period and age. These mutants did not have significant changes in body weight compared to control littermates during the 8 weeks of diet restriction; however, the release of this diet restriction resulted in a rapid weight increase (Figure 2H).

Dual-energy X-ray absorptiometry (DXA) analysis of mice 14–16 weeks after tamoxifen administration indicated that both Kif3a-cKO males and females had significant increases in fat mass and percentage fat when fed

*Correspondence: byoder@uab.edu

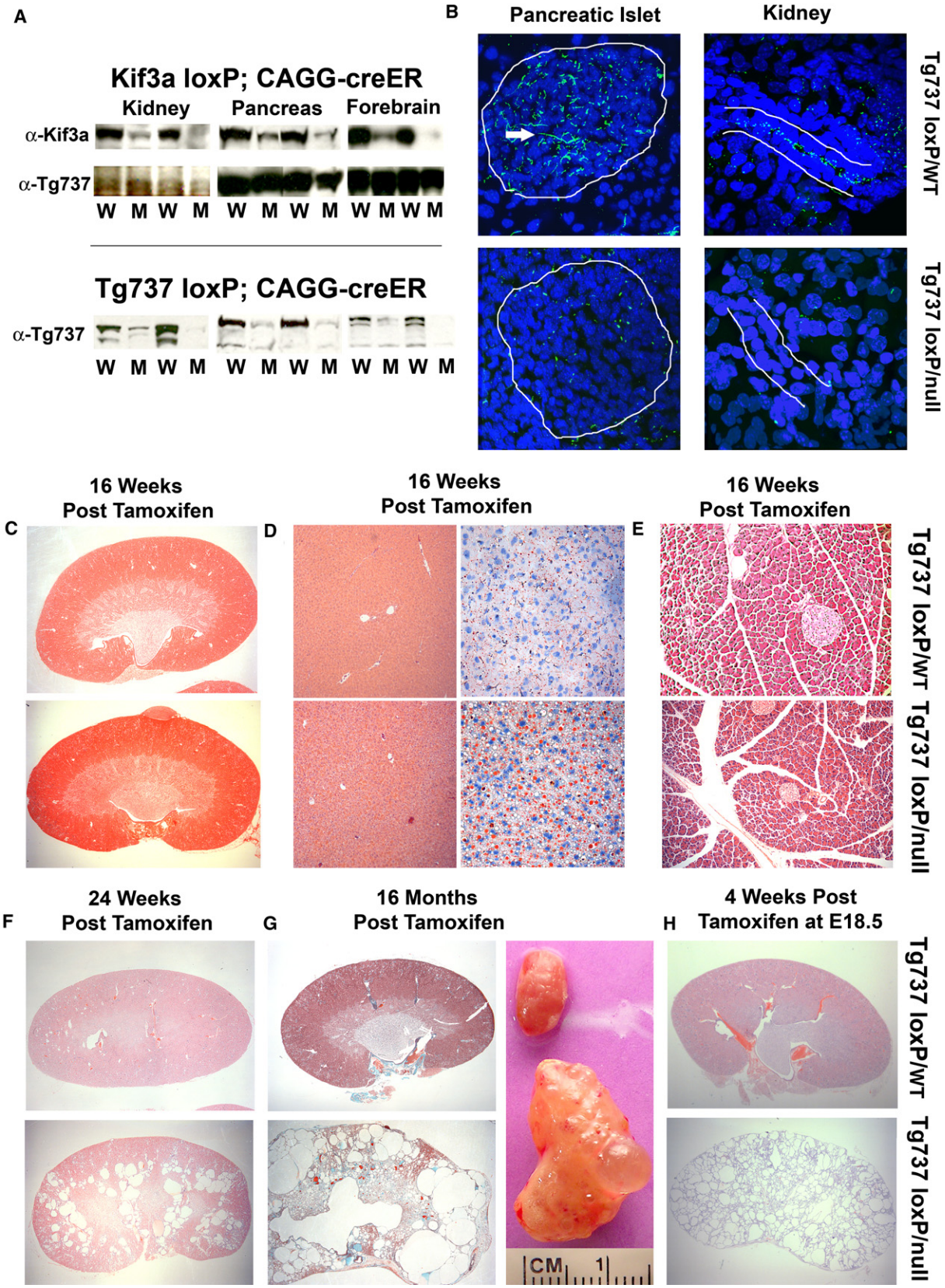

Figure 1. Systemic Conditional Deletion of Kif3a and Tg737 in Adult Mice Leads to the Development of Slow-Onset Cystic Kidney Disease

(A) Western-blot analysis of KIF3A protein in kidney, pancreas, and brain in *Kif3a*$^{loxP/wt}$; CAGG-creER (W) and *Kif3a*$^{loxP/null}$; CAGG-creER (M) animals 16 weeks after tamoxifen administration (top panel). TG737 protein expression (middle) was used as a loading control. TG737 protein expression was also measured in *Tg737*^{loxP}; *CAGG-creER*^{TM} mutant (M) and control (W) kidney, pancreas, and brain (bottom panel).

ad libitum, whereas only minimal increases were seen in pair-fed mutants (Figure 3A, Figure S1D). Postmortem carcass analysis indicates that this gain in fat mass in ad libitum-fed mutants was observed across all fat pads examined (Figure 3B, Figure S1E). Increased lean mass was also detected in Kif3a-cKO female mice (Figure S1D); however, these changes were not seen after pair feeding.

The "systemic" loss of cilia in *Kif3a*$^{loxP/null}$ and *Tg737*$^{loxP/null}$ mutants fed ad libitum also resulted in elevated levels of leptin, as well as elevated fasting serum glucose and insulin, similar to type II diabetes (Figures 3C–3E and Figures S2A–S2C). Levels of these hormones as well as fasting glucose were not elevated in pair-fed mutants, indicating that the phenotype is a consequence of the obesity rather than a direct effect of cilia dysfunction.

In addition to increased adiposity, there were changes in organ weights in Kif3a-cKO mice after tamoxifen administration (Table 1). In ad libitum-fed mutants (16 weeks after tamoxifen injection), the livers and kidneys were nearly double the weight of controls. This was not seen in any of the pair-fed mice, indicating that these phenotypes are a secondary consequence of the obesity and not due directly to the loss of cilia. The increase in liver weight in the ad libitum-fed mutants was associated with lipid accumulation, as reveled by oil red O staining (hepatic steatosis, Figure 1D, Figures S2E–S2F). Histological analysis indicates that the increased kidney weight at 16 weeks after injection in the obese mice was not due to the increased cystogenesis specifically in the ad libitum-fed Kif3a-cKO mutants.

The hyperphagia-induced obesity observed after tamoxifen administration in adult mice raised the possibility the abnormal feeding behavior might be due to the loss of ciliary function on neurons. To test this hypothesis, we crossed the conditional cilia mutants with the *synapsin1-cre* (*Syn1-cre*) mice. Although it did not occur as rapidly as seen for the *CAGG-CreER*^{TM} line, both male and female cilia mutants generated with *Syn1-cre* become obese (Figure 4). The cause of the delayed phenotype relative to what is seen in the *CAGG-CreER*^{TM}-induced mutants is uncertain but might reflect differences in the efficacy of the *Syn1-Cre* or possibly indicate additional roles for cilia in energy homeostasis outside of the central nervous system (CNS).

To further define on which neurons cilia function is needed, we disrupted cilia on pro-opiomelanocortin (POMC)-expressing cells in the hypothalamus. We accomplished this by crossing the *Kif3a* conditional mutant with the *POMC-cre* deletor line [16, 17]. To determine whether cilia were present on POMC neurons, we first crossed the *Kif3a* flox allele onto the cre reporter strain *Z/EG*. These mice were used for the generation of the conditional mutant and control mice. Cilia were detected by immunofluorescence analysis with an antibody to monoglycylated tubulin [18] and the POMC neurons by GFP expression. The data confirm that there is a single cilium present on most if not all POMC neurons (green fluorescent protein [GFP] positive) as well as most other cells in the hypothalamus (Figure 5A). In contrast, cilia were largely absent from the GFP-positive POMC neurons in the conditional mutants, whereas non-GFP-positive cell types in the hypothalamus retain a cilium (Figure 5B). Cilia were also retained in other regions of the brain outside of the hypothalamus in these mutants (data not shown) where *POMC-cre* is not expressed. Importantly, both male and female *Kif3a*$^{loxP/null}$*; POMC-cre* (hereafter called Kif3a-pomcKO) mice exhibited a significant increase in weight compared to their sex- and age-matched controls (Figure 5C). As seen for the *CAGG-CreER*^{TM} or *Syn1-cre* line, the obesity was due primarily to hyperphagia (Figure 5D and data not shown). In addition, the level of hyperphagia and obesity in the *POMC-cre* mice was not as remarkable as seen in the *CAGG-creER* mice. It is unlikely that the phenotype is caused by a loss of POMC neurons because we could detect no overt changes in the number of GFP-positive cells in the hypothalamus of the mutants on the *Z/EG* reporter background (Figures 5A and 5B). Another possible mechanism that could cause the obesity phenotype would be a change in activity. However, our analysis of the day-night movement patterns of male and female Kif3a-pomcKO mutants revealed no overt differences from that in controls (Figures S3A–S3B).

As seen with the *CAGG-CreER* line, DXA analysis revealed that the Kif3a-pomcKO mutants had a significant increase in percentage body fat and an increase in lean mass (Figure 5E). The increase in lean mass is likely to be a secondary effect of the increased adiposity or due to a small increase in linear growth (Figure 5F). Kif3a-pomcKO mice also had elevated levels of serum leptin and insulin and slightly higher blood glucose (Figures 5G–5I). Oil red O staining again revealed hepatic steatosis. As seen with the conditional mutants generated with the *CAGG-CreER*^{TM} line, the hepatic steatosis is a secondary effect of the obesity because this phenotype is not seen in pair-fed mutants, and *POMC-cre* is not expressed in the liver (Figures S3E–S3F).

(B) Confocal immunofluorescence analysis of Tg737-cWT and cKO tissues demonstrates the loss of cilia in the pancreatic islet (left panels; 63×; Tg737-cWT above, Tg737-cKO below) and in the nephrons of the kidney (right; 100×; Tg737-cWT above, Tg737-cKO below). The islet and tubule are roughly outlined in white. The longer green staining pattern (pointed at by tip of a white arrowhead) is due to the background of the secondary antibody, which reacts with an antigen on the vasculature and is unrelated to cilia.
(C–E) Hematoxylin and Eosin (H&E) staining of Tg737-cWT (top) and Tg737-cKO (bottom) kidney (C), liver ([D], left panels), and pancreas (E) at 16 weeks after tamoxifen administration in ad libitum-fed mice shows no cystic pathology or bile, and pancreatic-duct-related pathologies typical of the hypomorphic mutants at this age. Oil red O staining ([D], right panels) shows an increase in lipid (red stain) accumulation in the mutants.
(F) H&E staining of Tg737-cWT (top) and Tg737-cKO (bottom) kidneys at 24 weeks after tamoxifen injection in ad libitum-fed mice revealed the development of cysts in Tg737-cKO mice (bottom).
(G) Trichrome staining of Tg737-cWT (top) and Tg737-cKO (bottom) kidney sections 16 months after tamoxifen administration in ad libitum-fed mice reveals the presence of very large cystic lesions throughout the kidney of the conditional mutants. The gross appearance of age- and sex-matched kidneys from Tg737-cWT (top) and Tg737-cKO (bottom) are shown in the right panel.
(H) H&E Staining of Tg737-cWT (top) and Tg737-cKO (bottom) kidney sections 4 weeks after the administration of tamoxifen to the pregnant mother at embryonic day 18.5.

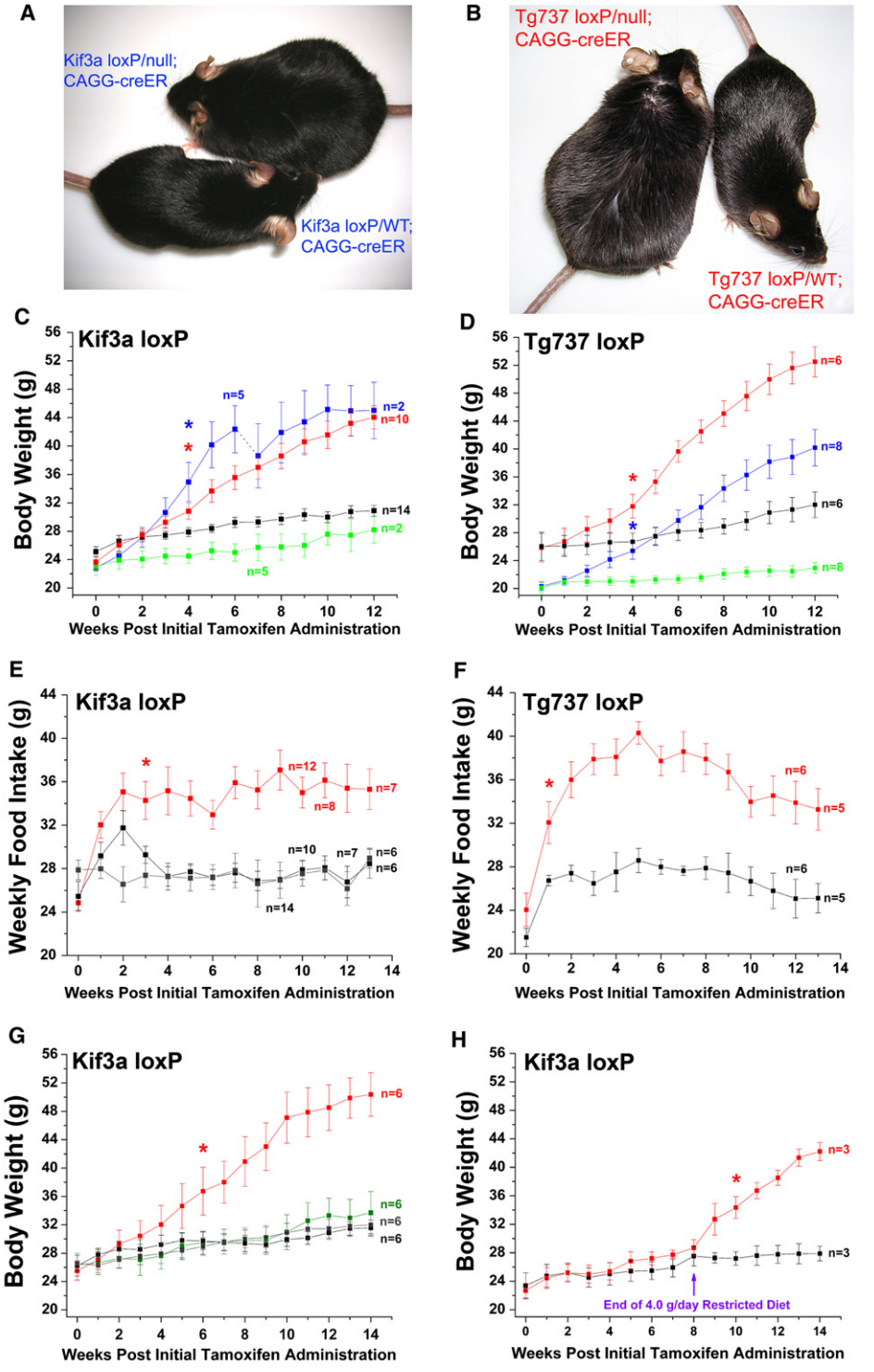

Figure 2. Systemic Loss of Kif3a and/or Tg737 from Adult Mice Results in a Hyperphagia-Induced Obesity Phenotype

(A) Images of Kif3a-cKO (left) and Kif3a-cWT (right) females 16 weeks after administration of tamoxifen. These littermates were of equivalent weight at time of injection.

(B) Tg737-cKO (left) and Tg737-cWT (right) females are also shown 16 weeks after tamoxifen administration.

(C and D) Body-weight analysis of Kif3a-cWT and Kif3a-cKO (C) and Tg737-cWT and Tg737-cKO (D) males and females after the tamoxifen administration (week 0). The number of Kif3a-cKO and Kif3a-cWT females analyzed in this study changed at week 6, when several of the mice were used to evaluate fat pad and organ weight masses. Animals were 8–12 weeks of age at the time of the initial tamoxifen administration.

(E and F) Weekly food intake analysis of Kif3a-cKO and Kif3a-cWT males (E) and Tg737-cKO and Tg737-cWT (F) males after the initial tamoxifen

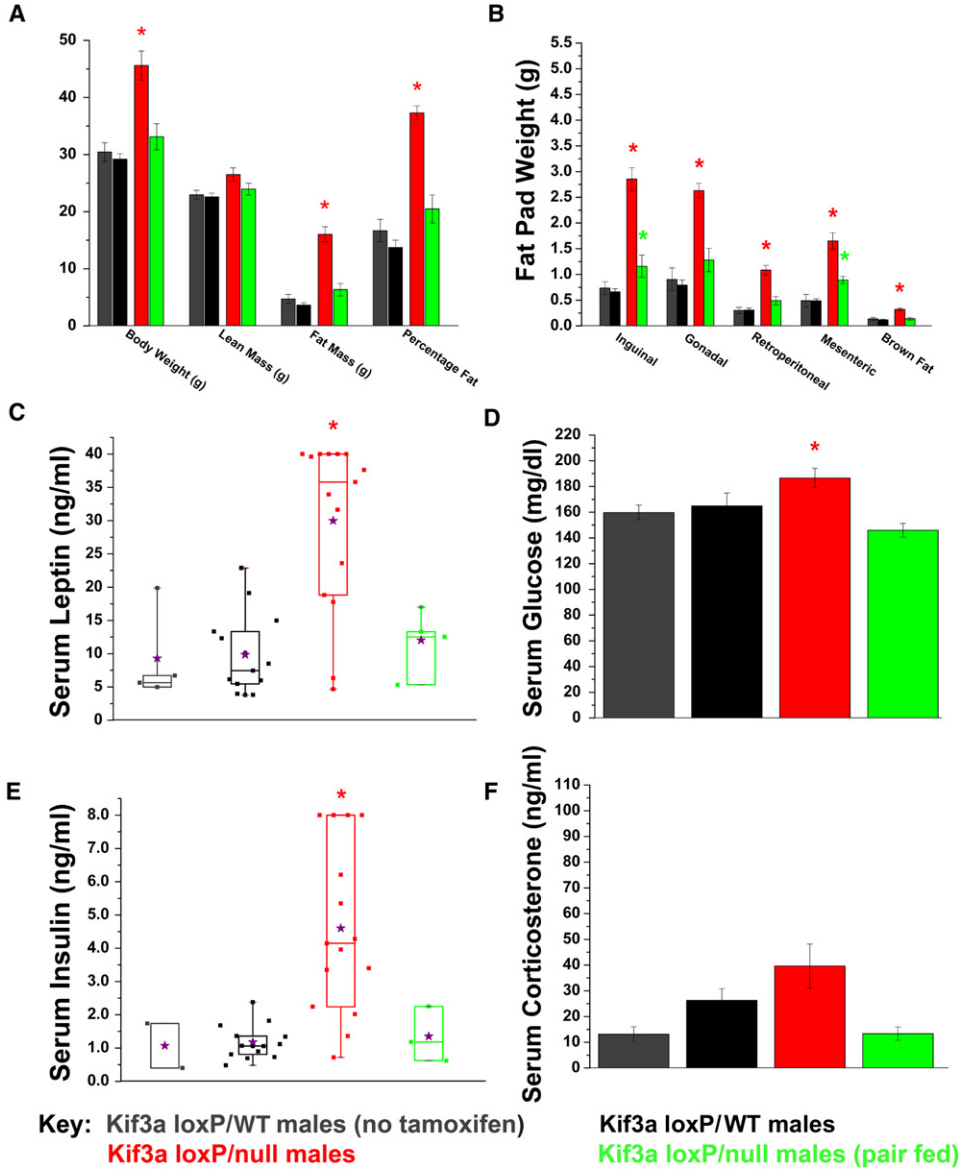

Figure 3. Body Composition and Serum Analysis of the Obesity Phenotype Displayed in Kif3a-cKO Males

(A) Dual energy X-ray absorptiometry (DXA) displaying lean mass, fat mass, and percentage body fat of male Kif3a-cWT and Kif3a-cKO mice 14 weeks after the initial tamoxifen administration. Body weight was measured immediately after the DXA.

(B) Carcass analysis of various fat pads and brown fat in Kif3a-cWT and Kif3a-cKO males 16 weeks after the initial tamoxifen administration.

(C) Box and whisker plot of nonfasting serum leptin levels in Kif3a-cWT and KO males 16 weeks after the initial tamoxifen administration. Eight out of then Kif3a-cKO ad libitum-fed mice were above the maximum threshold of detection (40 ng/ml) and were assigned a value of 40 ng/ml. Mean serum leptin levels are indicated by purple stars.

(D) Serum glucose analysis of Kif3a-cWT and Kif3a-cKO males measured after 4 hr of fasting conditions.

(E) Box and whisker plot of nonfasting serum insulin analysis of Kif3a-cWT and Kif3a-cKO males. Four out of 15 Kif3a-cKO males reached the highest detectable threshold for serum insulin analysis and were assigned the value of 8.0 ng/ml for statistical analysis.

(F) Serum corticosterone analysis shows no significant differences between Kif3a-cWT and Kif3a-cKO males.

"*" indicates $p \leq 0.05$ in (C) and (E); the means are indicated by purple stars. Error bars indicate the SD.

administration (week 0). Several animals were euthanized in the course of the experiment for body-composition and histological analyses. Kif3a-cWT controls that were not induced with tamoxifen are also shown in blue (E).

(G) Body-weight analysis in pair-feeding studies of Kif3a-cKO males after the administration of tamoxifen. Separate groups of Kif3a-cWT males were tested with or without tamoxifen so that changes due to tamoxifen administration could be assessed.

(H) Kif3a-cWT and Kif3a-cKO males were administered tamoxifen and were diet restricted to 4.0 g/day for 8 subsequent weeks. At 8 weeks, all mice were then fed ad libitum.

"*" indicates $p \leq 0.05$ and shows the initial point of significant deviation between controls and mutants. Error bars indicate the standard deviation (SD).

Table 1. Organ Weights in Pair-Fed and Ad Libitum-Fed Cilia Mutant Mice

	Ad Libitum Fed			Pair Fed
Tissue or Organ	Kif3a loxP/WT CAGG-CreER Females (no tamoxifen, n = 4)	Kif3a loxP/WT CAGG-CreER Females (tamoxifen, n = 4)	Kif3a loxP/null CAGG-CreER Females (tamoxifen, n = 4)	Kif3a loxP/null CAGG-CreER Females (tamoxifen, n = 4)
Liver	1.266 ± 0.067	1.319 ± 0.067	2.424 ± 0.295[a]	1.275 ± 0.143
Kidney	0.292 ± 0.017	0.300 ± 0.016	0.730 ± 0.295[a]	0.325 ± 0.018
Pancreas	0.152 ± 0.005	0.151 ± 0.017	0.187 ± 0.011	0.146 ± 0.020
Heart	0.132 ± 0.006	0.142 ± 0.008	0.167 ± 0.008[a]	0.116 ± 0.007[a]
Ovary	0.011 ± 0.001	0.013 ± 0.001	0.014 ± 0.001	0.014 ± 0.002
Lung	0.213 ± 0.025	0.227 ± 0.011	0.257 ± 0.033	0.196 ± 0.024

[a] Organ weight significantly different compared to controls ($p < 0.05$).

Discussion

Cilia function is thought to be required for normal renal physiology, as evidenced by the fact that the disruption of cilia specifically in the developing kidney results in severe cystic disease [1, 19]. Renal cilia have been shown to function as mechanosensors that detect fluid movement through the lumen of the nephron, and the loss of this mechanosensory activity is thought to be a key factor leading to cystogenesis [5–7]. Thus, it was surprising that the rate of cyst formation was so attenuated after cilia were ablated in the adult mice compared to what occurs in the perinatal period. The difference in the cystic phenotype is not due to limited cre activity because immunofluorescence and western-blot analysis demonstrate a dramatic loss of cilia on renal tubules along with a reduction in KIF3A and TG737 protein levels well before the cystic pathology develops. The cause of the switch from a very aggressive cystic disorder in cilia mutants induced during renal development to a mechanism of slow cyst formation in adult is still being assessed. It remains a formal possibility that the large kidney cysts that develop in the adult induced mutants at 16 months after tamoxifen injection are related to the severity of obesity, as is the case for the hepatic steatosis and glucose homeostasis abnormalities. We are currently addressing this issue by using a kidney-specific tamoxifen-inducible Cre line. Overall, we believe the data indicate that renal cyst formation, as is likely the case for the pancreatic and hepatic ductile abnormalities associated with the cilia mutants such as *Tg737*^{orpk} [13, 14, 20], requires more than just the loss of a pathway regulated by cilia-mediated mechanosensation.

In addition, our data show that the loss of cilia in adult mice alters their feeding behavior and results in obesity with a phenotype resembling insulin resistance and diabetes. Obese mutants also exhibit renal hypertrophy, which is seen in diabetic mouse models and human patients [21, 22]. We further demonstrate that the obesity phenotype can largely be recapitulated by the deletion of cilia on neurons throughout the CNS and, more specifically, on POMC-expressing cells. Although *POMC-cre* is also expressed in the pituitary, it is likely that the phenotype is due to the loss of cilia function in hypothalamic POMC neurons. This is based on the fact that an obesity phenotype is also seen in cilia mutants generated with the *Syn1-cre* line [23]. Furthermore, we analyzed corticosterone levels in obese and pair-fed mutants that would probably be associated with affects on the pituitary and detected no significant differences or correlations between obese and nonobese mutant or control mice (Figure 3F and Figures S3D and S4G). Together, these data argue against cilia dysfunction on cells in the anterior pituitary as being the cause of the obesity.

Another interesting observation is that the phenotype of the cilia mutants generated with the *POMC-* or *Syn1-cre* lines are not as severe as that seen when cilia loss is induced systemically in adults. This could reflect a difference in the efficacy or time of expression of these cre lines or the possibility that cilia have additional roles in energy balance outside of the CNS. Another possibility is that neuronal feeding circuits are able to compensate for the congenic loss of cilia function during development but lack this capacity in adults after the disruption of cilia.

Mutations in several cilia- or basal-body-localized proteins have been implicated in rare human obesity syndromes such as Alström (ALMS) and Bardet-Biedl (BBS) [8, 24]. There are multiple proteins involved in BBS, and recent data indicate that they function as

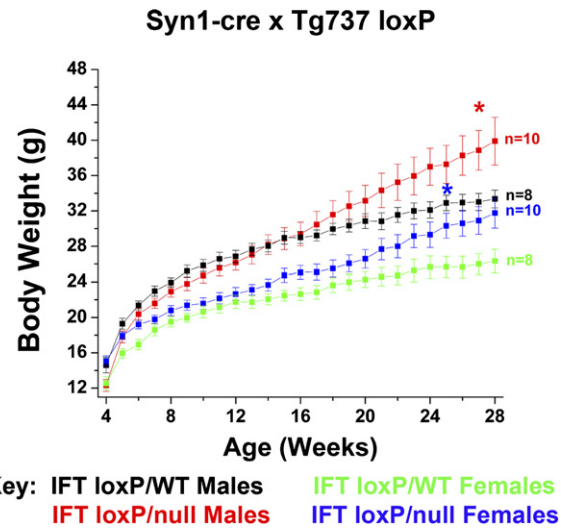

Figure 4. Conditional Disruption of *Tg737* in Neurons

Body weights of Tg737-Syn1KO and Tg737-Syn1WT male and female mice indicate that the loss of neuronal cilia because of the disruption of *Tg737* results in an obese phenotype. Error bars indicate the standard deviation.

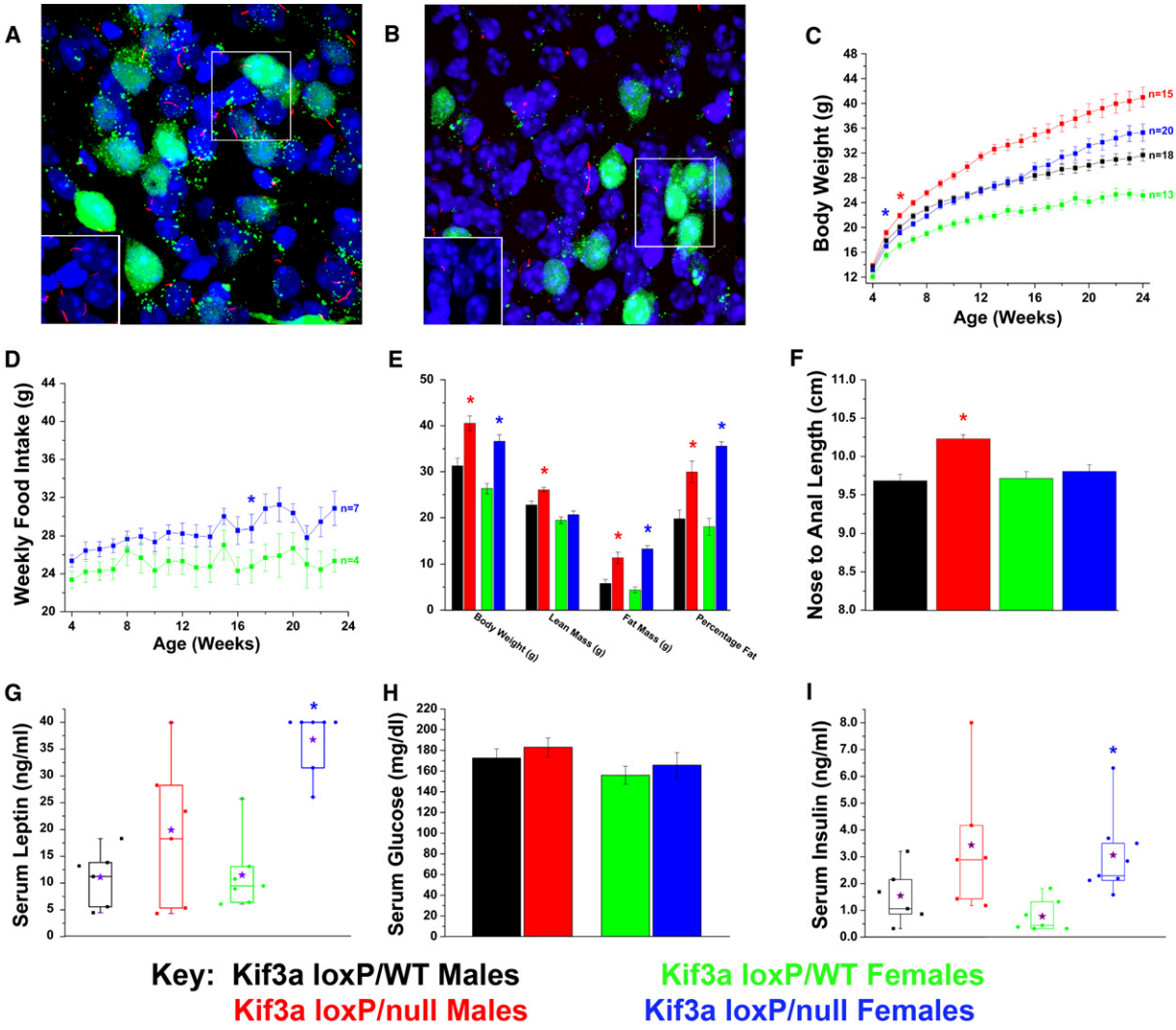

Figure 5. Conditional Deletion of Kif3a from POMC-Expressing Cells in Mice Leads to Increases in Weight, Adiposity, and Body Length

(A and B) Confocal immunofluorescence analysis of *Kif3a*$^{loxP/wt}$ (Kif3a-pomcWT) (A) and *Kif3a*$^{loxP/null}$ (Kif3a-pomcKO) (B) arcuate nucleus (100×) bred onto the *Z/EG* Cre reporter line in the presence of the *POMC-cre* deletor strain demonstrates the loss or stunting of neuronal cilia (red) on affected POMC neurons (green). Inserts show cilia (red) without the GFP signal and are derived from the boxed region in the image. Note that cilia are still retained on the non-POMC-expressing cells in the hypothalamus.

(C) Body-weight analysis of Kif3a-pomcKO and Kif3a-pomcWT males and females.

(D) The weekly food intake of Kif3a-pomcKO females was consistently increased from that of the Kif3a-pomcWT controls.

(E) DXA analysis performed on adult (age 22–25 weeks) mice showed significant increases in fat mass and percentage fat in both sexes and lean mass in male Kif3a-pomcKO mice. Body weight was measured after the DXA analysis.

(F) Nose-to-anal length analysis conducted in anesthetized adult (age 22–25 weeks) Kif3a-pomcWT and Kif3a-pomcKO mice. The average length from independently determined two blinded measurements was used.

(G–I) Serum analysis of nonfasted leptin (G), 4 hr fasted glucose (H), and nonfasted insulin (I) in Kif3a-pomcWT and Kif3a-pomcKO mice.

"*" indicates $p \leq 0.05$ in (C) and (D) and shows the initial point of significant deviation between controls and mutants. The purple stars in (G) and (I) represent the means of the individual groups. Error bars indicate the SD.

a complex to regulate vesicular transport to the cilium [24]. The ALMS1 protein, which is involved in human Alström syndrome, is also located at the base of the cilium, and the disruption of ALMS1 caused the truncation of the cilium [22]. Recently, another gene involved in the obesity and skeletal defects observed in human patients with Carpenter Syndrome was identified as *Rab23* [25]. RAB23 is a negative regulator of the hedgehog pathway that functions downstream of the hedgehog receptors Smoothened and Patched, as well as cilia and/or IFT proteins such as TG737 (IFT88). Although the pathway disrupted in Carpenter Syndrome patients or in which the tissue loss of RAB23 leads to the obesity phenotype is unknown, these recent data raise the possibility that the increased adiposity in our conditional cilia mutants might be related to abnormalities in hedgehog signaling. Overall, these data are supportive of a role for the ciliary and/or basal body in regulating feeding behavior. The control of feeding in mammals is complex and involves signals from diverse tissues, such as the intestine, pancreas, adipose, and stomach [26, 27]. In many cases, these signals converge on the CNS and

particularly on neurons in the hypothalamus. Our data are consistent with a role for cilia on the hypothalamic POMC neurons in the reception or response to a satiety signal such as leptin or insulin, and suggest that this might be disrupted in the BBS or ALMS patients. An alternative possibility is that cilia are involved in a pathway connecting POMC neuronal projections to known reward circuitry in regions of the brain such as the ventral tegmental area, as recently proposed for leptin and its receptor [27, 28]. As such, our data provide a more comprehensive assessment of the cellular mechanisms controlling food intake in mammals and could provide novel insights into one of the central satiety pathways in humans.

Supplemental Data

Experimental Procedures and three figures are available at http://www.current-biology.com/cgi/content/full/17/18/1586/DC1/.

Acknowledgments

We would like to thank Maria S. Johnson from the University of Alabama at Birmingham (UAB) Small Animal Phenotyping Core for her assistance with the carcass analyses, Jinju Zhang from the UAB Transgenic Mouse Facility for his help with serum collection, and Barbara A. Gower and Maryellen Williams from the UAB Energy Metabolism and Body Composition Core for their help on the serum analyses. We would also like to thank Maya Watts, Jane Hosmer, and Camille Effler from the UAB Comparative Pathology Core for their technical support. We also would like to acknowledge M.H. Bré for her generosity in providing TAP952 antibody. B.K.Y. is supported by National Institutes of Health (NIH) R01DK65655, NIH R56DK075996, and the UAB Clinical Nutrition Research Center Pilot and Feasibility Project Grant. T.R.N. and the UAB Small Animal Phenotyping Core are supported by UAB Clinical Nutrition Research Unit, P30DK56336, and the Alabama Neuroscience Blueprint Core Center, P30NS057098. R.A.K. is supported by NIH DK58382 and by NIH P30 CA13148 to the UAB Transgenic Mouse Facility. The UAB behavioral core is supported in part by NIH P30 NS47466.

Received: July 3, 2007
Revised: August 3, 2007
Accepted: August 6, 2007
Published online: September 6, 2007

References

1. Lin, F., Hiesberger, T., Cordes, K., Sinclair, A.M., Goldstein, L.S., Somlo, S., and Igarashi, P. (2003). Kidney-specific inactivation of the KIF3A subunit of kinesin-II inhibits renal ciliogenesis and produces polycystic kidney disease. Proc. Natl. Acad. Sci. USA *100*, 5286–5291.
2. Marszalek, J.R., Ruiz-Lozano, P., Roberts, E., Chien, K.R., and Goldstein, L.S. (1999). Situs inversus and embryonic ciliary morphogenesis defects in mouse mutants lacking the KIF3A subunit of kinesin-II. Proc. Natl. Acad. Sci. USA *96*, 5043–5048.
3. Murcia, N.S., Richards, W.G., Yoder, B.K., Mucenski, M.L., Dunlap, J.R., and Woychik, R.P. (2000). The Oak Ridge Polycystic Kidney (orpk) disease gene is required for left-right axis determination. Development *127*, 2347–2355.
4. Singla, V., and Reiter, J.F. (2006). The primary cilium as the cell's antenna: Signaling at a sensory organelle. Science *313*, 629–633.
5. Praetorius, H.A., and Spring, K.R. (2003). The renal cell primary cilium functions as a flow sensor. Curr. Opin. Nephrol. Hypertens. *12*, 517–520.
6. Nauli, S.M., Alenghat, F.J., Luo, Y., Williams, E., Vassilev, P., Li, X., Elia, A.E., Lu, W., Brown, E.M., Quinn, S.J., et al. (2003). Polycystins 1 and 2 mediate mechanosensation in the primary cilium of kidney cells. Nat. Genet. *33*, 129–137.
7. Al-Bhalal, L., and Akhtar, M. (2005). Molecular basis of autosomal dominant polycystic kidney disease. Adv. Anat. Pathol. *12*, 126–133.
8. Li, G., Vega, R., Nelms, K., Gekakis, N., Goodnow, C., McNamara, P., Wu, H., Hong, N.A., and Glynne, R. (2007). A Role for Alstrom Syndrome Protein, Alms1, in Kidney Ciliogenesis and Cellular Quiescence. PLoS Genet. *3*, e8.
9. Davenport, J.R., and Yoder, B.K. (2005). An incredible decade for the primary cilium: A look at a once-forgotten organelle. Am. J. Physiol. Renal Physiol. *289*, F1159–F1169.
10. Takeda, S., Yonekawa, Y., Tanaka, Y., Okada, Y., Nonaka, S., and Hirokawa, N. (1999). Left-right asymmetry and kinesin superfamily protein KIF3A: New insights in determination of laterality and mesoderm induction by kif3A−/− mice analysis. J. Cell Biol. *145*, 825–836.
11. Hayashi, S., and McMahon, A.P. (2002). Efficient recombination in diverse tissues by a tamoxifen-inducible form of Cre: a tool for temporally regulated gene activation/inactivation in the mouse. Dev. Biol. *244*, 305–318.
12. Haycraft, C.J., Zhang, Q., Song, B., Jackson, W.S., Detloff, P.J., Serra, R., and Yoder, B.K. (2007). Intraflagellar transport is essential for endochondral bone formation. Development *134*, 307–316.
13. Banizs, B., Pike, M.M., Millican, C.L., Ferguson, W.B., Komlosi, P., Sheetz, J., Bell, P.D., Schwiebert, E.M., and Yoder, B.K. (2005). Dysfunctional cilia lead to altered ependyma and choroid plexus function, and result in the formation of hydrocephalus. Development *132*, 5329–5339.
14. Zhang, Q., Davenport, J.R., Croyle, M.J., Haycraft, C.J., and Yoder, B.K. (2005). Disruption of IFT results in both exocrine and endocrine abnormalities in the pancreas of Tg737(orpk) mutant mice. Lab. Invest. *85*, 45–64.
15. Pazour, G.J., Dickert, B.L., Vucica, Y., Seeley, E.S., Rosenbaum, J.L., Witman, G.B., and Cole, D.G. (2000). Chlamydomonas IFT88 and its mouse homologue, polycystic kidney disease gene tg737, are required for assembly of cilia and flagella. J. Cell Biol. *151*, 709–718.
16. Xu, A.W., Kaelin, C.B., Takeda, K., Akira, S., Schwartz, M.W., and Barsh, G.S. (2005). PI3K integrates the action of insulin and leptin on hypothalamic neurons. J. Clin. Invest. *115*, 951–958.
17. Novak, A., Guo, C., Yang, W., Nagy, A., and Lobe, C.G. (2000). *Z/EG*, a double reporter mouse line that expresses enhanced green fluorescent protein upon Cre-mediated excision. Genesis *28*, 147–155.
18. Bre, M.H., Redeker, V., Vinh, J., Rossier, J., and Levilliers, N. (1998). Tubulin polyglycylation: differential posttranslational modification of dynamic cytoplasmic and stable axonemal microtubules in paramecium. Mol. Biol. Cell *9*, 2655–2665.
19. Yoder, B.K., Mulroy, S., Eustace, H., Boucher, C., and Sandford, R. (2006). Molecular pathogenesis of autosomal dominant polycystic kidney disease. Expert Rev. Mol. Med. *8*, 1–22.
20. Yoder, B.K., Richards, W.G., Sweeney, W.E., Wilkinson, J.E., Avener, E.D., and Woychik, R.P. (1995). Insertional mutagenesis and molecular analysis of a new gene associated with polycystic kidney disease. Proc. Assoc. Am. Physicians *107*, 314–323.
21. Satriano, J. (2007). Kidney growth, hypertrophy and the unifying mechanism of diabetic complications. Amino Acids *33*, 331–339.
22. Lee, M.J., Feliers, D., Mariappan, M.M., Sataranatarajan, K., Mahimainathan, L., Musi, N., Foretz, M., Viollet, B., Weinberg, J.M., Choudhury, G.G., and Kasinath, B.S. (2007). A role for AMP-activated protein kinase in diabetes-induced renal hypertrophy. Am. J. Physiol. Renal Physiol. *292*, F617–F627.
23. Zhu, Y., Romero, M.I., Ghosh, P., Ye, Z., Charnay, P., Rushing, E.J., Marth, J.D., and Parada, L.F. (2001). Ablation of NF1 function in neurons induces abnormal development of cerebral cortex and reactive gliosis in the brain. Genes Dev. *15*, 859–876.
24. Nachury, M.V., Loktev, A.V., Zhang, Q., Westlake, C.J., Peranen, J., Merdes, A., Slusarski, D.C., Scheller, R.H., Bazan, J.F., Sheffield, V.C., and Jackson, P.K. (2007). A Core Complex of BBS Proteins Cooperates with the GTPase Rab8 to Promote Ciliary Membrane Biogenesis. Cell *129*, 1201–1213.
25. Jenkins, D., Seelow, D., Jehee, F.S., Perlyn, C.A., Alonso, L.G., Bueno, D.F., Donnai, D., Josifiova, D., Mathijssen, I.M., Morton, J.E., et al. (2007). RAB23 mutations in Carpenter syndrome imply an unexpected role for hedgehog signaling in cranial-suture development and obesity. Am. J. Hum. Genet. *80*, 1162–1170.

26. Badman, M.K., and Flier, J.S. (2005). The gut and energy balance: Visceral allies in the obesity wars. Science *307*, 1909–1914.
27. Fulton, S., Pissios, P., Manchon, R.P., Stiles, L., Frank, L., Pothos, E.N., Maratos-Flier, E., and Flier, J.S. (2006). Leptin regulation of the mesoaccumbens dopamine pathway. Neuron *51*, 811–822.
28. Hommel, J.D., Trinko, R., Sears, R.M., Georgescu, D., Liu, Z.W., Gao, X.B., Thurmon, J.J., Marinelli, M., and DiLeone, R.J. (2006). Leptin receptor signaling in midbrain dopamine neurons regulates feeding. Neuron *51*, 801–810.